

Article

Establishment and Validation of Patient-Derived Non-Small Cell Lung Cancer Organoids as In Vitro Lung Cancer Models

Raphael S. Werner ^{1,*} , Jae-Hwi Jang ¹, Markus Rechsteiner ², Michaela B. Kirschner ¹  and Isabelle Opitz ¹ 

¹ Department of Thoracic Surgery, University Hospital Zurich, 8091 Zurich, Switzerland; jae_hwi.jang@usz.ch (J.-H.J.); michaela.kirschner@usz.ch (M.B.K.)

² Department of Pathology and Molecular Pathology, University Hospital Zurich, 8091 Zurich, Switzerland

* Correspondence: raphael.werner@usz.ch

Abstract: Background: Recent advances in the personalized treatment of non-small cell lung cancer (NSCLC) require representative in vitro model systems that reflect tumor heterogeneity and maintain the characteristic genetic aberrations. We therefore aimed to establish patient-derived NSCLC organoids that offer a reliable platform for further investigations. Methods: NSCLC organoids were cultured between May 2020 and February 2022 from surgically resected NSCLC tissue specimens. After histological and immunohistochemical validation, genetic validation was performed by targeted next-generation sequencing of tissue and organoid specimens using the OncoPrint Focus Assay (ThermoFisher Scientific). Results: From 37 resected NSCLC samples, 18 primary organoid cultures were successfully established and expanded during early passages. Upon histomorphological validation, organoids showed complementary characteristics when compared to the resected parental tumor, including adenocarcinoma, squamous cell carcinoma, mucoepidermoid carcinoma, and lung carcinoma differentiation. Among nine parental tumors, traceable genetic alterations were detected, and three corresponding organoids lines retained this mutational profile, including a KRAS p.Gly12Val mutation, KRAS p.Gly12Cys mutation, and RET-fusion. Conclusions: The establishment of primary NSCLC organoids from surgically resected tissue is feasible. Histological, immunohistochemical, and genetic validation is essential to identify representative NSCLC organoids that maintain the characteristics of the parental tumor. Overall, low establishment rates remain a challenge for broad clinical applications.

Keywords: non-small cell lung cancer; cancer organoids; cancer model; stem cells; intratumoral heterogeneity



Citation: Werner, R.S.; Jang, J.-H.; Rechsteiner, M.; Kirschner, M.B.; Opitz, I. Establishment and Validation of Patient-Derived Non-Small Cell Lung Cancer Organoids as In Vitro Lung Cancer Models. *Organoids* **2024**, *3*, 281–294. <https://doi.org/10.3390/organoids3040017>

Academic Editor: Süleyman Ergün

Received: 15 August 2024

Revised: 25 October 2024

Accepted: 28 October 2024

Published: 9 November 2024



Copyright: © 2024 by the authors. Licensee MDPI, Basel, Switzerland. This article is an open access article distributed under the terms and conditions of the Creative Commons Attribution (CC BY) license (<https://creativecommons.org/licenses/by/4.0/>).

1. Introduction

Lung cancer is the most common cause of cancer-related death worldwide, each year resulting in more than 36 million disability-adjusted life years globally [1]. Non-small cell lung cancer (NSCLC), the most common type of lung cancer, is a highly heterogeneous disease, both on a histological and on a molecular level. NSCLC has one of the highest tumor mutational burdens among all cancer types and therefore carries a broad variety of different somatic alterations and genomic rearrangements [2]. Furthermore, multiregional intratumor heterogeneity analyses demonstrate that molecular intratumoral heterogeneity and a branched cancer evolution are almost universally present in NSCLC [2]. For cancer research including biomarker studies or the assessment of personalized candidate cancer treatments, representative in vitro systems that reflect inter- and intratumoral heterogeneity and maintain the genetic characteristics of the parental tumor are essential. In the past few years, two-dimensional cell lines [3], genetically engineered mouse models [4], and patient-derived xenografts (PDXs) [5] have largely been used as preclinical models of NSCLC. Since common two-dimensional cancer cell lines do not generally maintain their original heterogeneity and three-dimensional structure, they are fundamentally limited in

representing the complexity of lung cancer [6]. And although PDX models are able to mimic the characteristics of the primary tumors including the mutational profile, intratumoral heterogeneity and tumor microenvironment, the development of cancer in these models is highly time-consuming, expensive, and entails animal testing [5]. As an alternative, patient-derived NSCLC organoids consist of a functional, three-dimensional cluster of stem cells and polyclonal cells that undergo self-organization and have therefore been suggested as alternative in vitro models that maintain the heterogeneous characteristics of the primary tumor [7]. Despite its high global disease burden, lung cancer is underrepresented in translational organoid research, and real-life data including establishment rates and validation are scarce [8–13].

In this study, we aimed to establish a culture protocol for patient-derived NSCLC organoids from fresh cancer tissue followed by subsequent histological and genetic validation.

2. Materials and Methods

2.1. Human NSCLC Tissue Specimens for Organoid Culture

Surgically resected NSCLC specimens of all stages were transferred from the operating theatre to the Department of Pathology for frozen section diagnosis. Spare tissue that was not required for further diagnostics was transported to the laboratory on ice within 2–3 h after resection. The study was performed in compliance with the institutional guidelines, and approval by the local ethics committee was obtained for the establishment and characterization of primary NSCLC cell cultures and the patients' clinical data obtained from within the standard clinical practice (BASEC-reference number: 2019-01313). All patients signed an informed consent form.

2.2. Tissue Processing and Culture of Patient-Derived NSCLC Organoids

Tissue specimens (sized $\sim 5 \text{ mm}^3$ – 3 cm^3) were washed three times in Dulbecco's phosphate-buffered saline (DPBS, PAN Biotech, Aidenbach, Germany). Subsequently, mechanical and enzymatic dissociation was performed (Figure 1). Specimens were sectioned into a homogenous mass using sterile blades and incubated with 1 mg/mL collagenase (Sigma-Aldrich, St. Louis, MO, USA) and 0.001% DNase (Sigma-Aldrich) for 45 min at 37 °C. After incubation, the suspension was passed through a 70 μm cell strainer and centrifuged at $550 \times g$ for 5 min. If a layer of red blood cells was visible in the pellet, it was resuspended in 1 mL red blood cell lysis buffer (150 mM ammonium chloride, 10 mM potassium hydrogen carbonate, and 130 μM EDTA in double-distilled water) for 5 min and re-centrifuged at $550 \times g$ for 5 min. The pellet was then resuspended in 125 μL serum-free organoid medium. A previously reported minimal medium formulation by Kim et al. [9] and Shi et al. [13] was further modified. For organoid culture, Advanced DMEM/F-12 (ThermoFisher Scientific, Waltham, MA, USA) was supplemented with 4 mM GlutaMAX (ThermoFisher Scientific, Waltham, MA, USA), 25 mM HEPES buffer (ThermoFisher Scientific, Waltham, MA, USA), 1% penicillin/streptomycin, 50 ng/mL human epidermal growth factor (hEGF, PeproTech), 50 ng/mL basic fibroblast growth factor (bFGF, PeproTech/ThermoFisher Scientific, Waltham, MA, USA), 1 X B-27 serum-free supplement (ThermoFisher Scientific, Waltham, MA, USA), 1% N-2 supplement (ThermoFisher Scientific, Waltham, MA, USA), 10 μM rho-kinase (ROCK) inhibitor Y-27632 (Enzo Life Sciences, Farmingdale, NY, USA), and 500 nM A83-01 (Stemcell Technologies, Vancouver, BC, Canada). The complete growth medium formulation is shown in Table 1. Then, 375 μL of pre-thawed Matrigel Matrix for Organoid Culture (Corning, Corning, NY, USA) was added to the 125 μL of cell-medium suspension. The suspension was immediately plated on pre-warmed, non-coated, 12-well culture plates (TPP) with 5 wells each holding 1 Matrigel dome of 100 μL . After gelation at 37 °C, 2 mL of organoid medium was added to each well, and culture plates were maintained in 37 °C and 5% CO_2 .

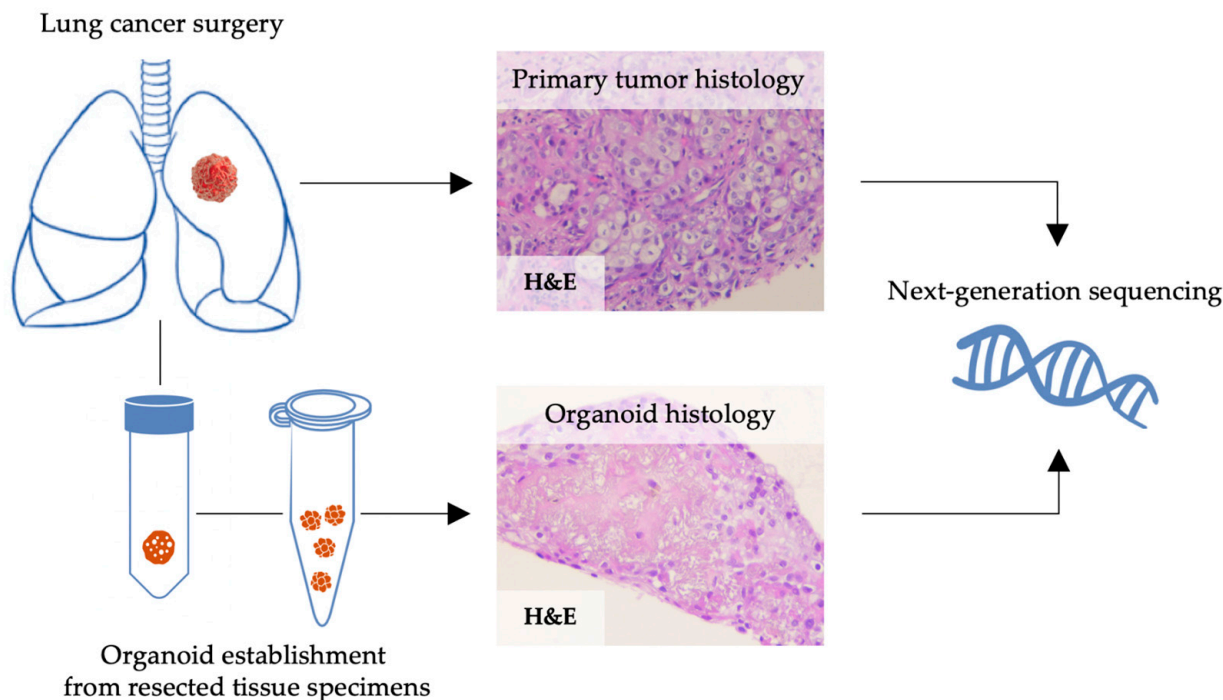


Figure 1. Schematic outline of the processing of fresh lung cancer tissue for culturing of primary NSCLC organoids. Tumor tissue was transferred to the laboratory, where it underwent mechanical and enzymatic digestion and was subsequently plated in 12-well plates.

Table 1. Culture medium formulation for the establishment of patient-derived non-small cell lung cancer organoids.

Additive	Final Concentration
Advanced DMEM/F12 (ThermoFisher)	
GlutaMax (ThermoFisher)	4 mM
HEPES Buffer (ThermoFisher)	25 mM
Penicillin/streptomycin (1%)	10 μ L/mL
Human epidermal growth factor (hEGF, PeproTech)	50 ng/mL
Basic fibroblast growth factor (bFGF, PeproTech)	50 ng/mL
B-27 serum-free supplement (ThermoFisher)	25 μ L/mL
N-2 supplement (ThermoFisher)	10 μ L/mL
rho-kinase (ROCK) inhibitor Y-27632 (Enzo Life Sciences)	10 μ M
A83-01 (Stemcell)	500 nM

The organoid growth pattern was monitored regularly and medium was changed every 4–10 days depending on growth rate. The organoids were passaged between 7 and 28 days after initial plating. For splitting, the supernatant was removed and the Matrigel drop was resuspended in 1 mL 1X TrypLE select (ThermoFisher) and incubated at 37 °C for 5–10 min under close surveillance for organoid dissociation. After dissociation, 5 mL ice-cold advanced DMEM/F12 containing 1X B-27 serum-free supplement was added to stop the digestion, and the suspension was centrifuged at 550 \times g for 5 min. The pellet was washed in 3 mL ice-cold DPBS and again centrifuged at 550 \times g for 5 min. Subsequently, the pellet was resuspended in organoid medium and Matrigel (1:3) and reseeded at ratios of 1:2 or 1:3. Histological, immunohistochemical, and genetic characterization was performed in early passages (1–4) as soon as sufficient organoids were available to ensure the continuation of organoid culture.

2.3. Histology and Immunohistochemistry (IHC) for Validation of Patient-Derived Organoids

Organoids were suspended in pooled fresh-frozen plasma and reconstituted thrombin. The resulting organoid block was fixed overnight in 4% buffered formalin, dehydrated, and embedded in paraffin. Hematoxylin–eosin (H&E) staining and IHC was performed on 2 µm paraffin-cut sections. According to the Best Practices Recommendations for Diagnostic Immunohistochemistry in Lung Cancer, a panel of Thyroid transcription factor-1 (TTF-1), p40 and panCK was used for subtyping NSCLC [14]. In neuroendocrine differentiation, Ki-67 staining and synaptophysin staining were additionally performed [14]. For IHC, paraffin-cut sections were deparaffinized and rehydrated, and staining for TTF-1 clone 8G7G3/1 (Agilent Dako, Basel, Switzerland), p40 clone BC28 (Abcam, Cambridge, UK), panCK clone AE1/AE3 (Agilent Dako, Basel, Switzerland), and CD44 clone DF1485 (Agilent Dako, Basel, Switzerland) was performed using a Dako Autostainer Link48 (Dako Denmark A/S, Glostrup, Denmark) according to the manufacturer's instructions. For antigen retrieval, target retrieval solution pH 6 (Dako, Agilent Dako, Basel, Switzerland) was used for p40, panCK, CD44 and TTF-1. Ki-67 staining and synaptophysin staining was performed using the fully automated Benchmark staining system (Ventana Medical Systems Inc., Oro Valley, AZ, USA) using primary antibodies against Ki-67, clone 30-09 (Ventana Medical Systems Inc., Oro Valley, AZ, USA), and synaptophysin, clone 27D12 (Novocastra, Newcastle, UK).

2.4. Next Generation Sequencing (NGS)

NGS was conducted using the Oncomine Focus Assay (OFA) panel (Thermo Fisher Scientific, Waltham, MA, USA), enabling detection of variants in 52 genes. Sample analysis and library construction were performed according to the manufacturer's protocol. DNA and RNA were extracted from paraffin-embedded organoid blocks with a Maxwell 16 FFPE Tissue LEV DNA/RNA Purification Kit (Promega, Fitchburg, WI, USA). Sequencing was performed using the Ion S5TM System and the Ion 540 Sequencing Kit (Thermo Fisher Scientific, Waltham, MA, USA). Ion Reporter software 5.10 (Thermo Fisher Scientific, Waltham, MA, USA) was used for alignment (hg19/GRCh37), variant calling, and annotations.

3. Results

3.1. Establishment of Patient-Derived NSCLC Organoids

Between May 2020 and February 2022, tissue specimens were obtained from 37 NSCLC patients who underwent surgical resection at the Department of Thoracic Surgery of the University Hospital Zurich. Out of 37 processed tissue samples, 18 NSCLC organoids were successfully established (Figure 2A, Table 2), including 10 AC organoids from 20 AC specimens, 5 SCC organoids from 12 SCC specimens, 2 pulmonary carcinoid tumor organoids and 1 organoid from a mucoepidermoid carcinoma. Established organoids originated from all stages of NSCLC, including seven UICC (8th edition, 2017) stage I tumors, six stage II tumors, three stage III tumor and two stage IV tumors (Table 2, Supplementary Table S1). Among patients with established organoids, the mean age was 67.7 ± 9.7 years, 10 patients (55.5%) were male, and 2 patients (11.1%) had received neoadjuvant treatment. The mean diameter of the specimens received for culture was 9.2 ± 4.0 mm in cases with a successful establishment and 8.0 ± 4.1 mm in cases with a failed establishment (Supplementary Table S1). Different growth patterns were seen upon expansion in Matrigel (Figure 2B); while most organoids formed round shapes with increasing diameter over time, certain organoids showed extending prongs infiltrating into the surrounding Matrigel. Other organoids eventually attached to the culture plate and expanded by two-dimensional growth. In the latter cases, organoid formation could be re-established after splitting and resuspending the cells in Matrigel. Following a learning curve, establishment rates and the duration of expansion increased over time, resulting in an intermediate-term culture over up to 10 passages and 2–3 months in the latest samples (Figure 2C).

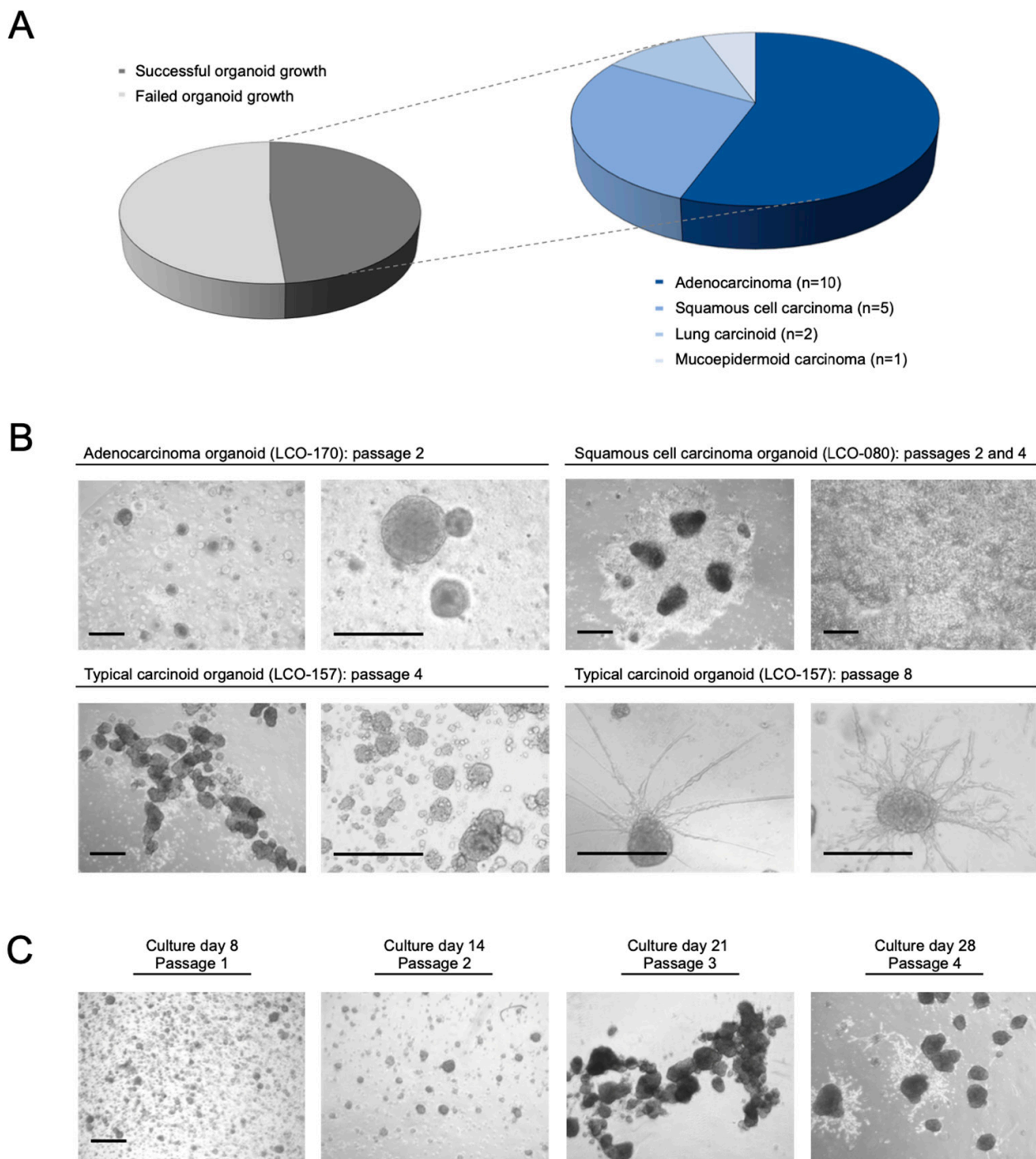


Figure 2. Primary NSCLC organoids established from fresh cancer tissue. **(A):** Out of 37 processed tissue samples, successful organoid growth was achieved in 18 cases. **(B):** Organoids commonly grew in round shapes with increasing diameter, as depicted in the brightfield microscopy images from adenocarcinoma organoids (LCO-170) and typical carcinoid organoids (LCO-157). Other organoids featured adherent growth, as seen in the brightfield microscopy images from squamous cell carcinoma (LCO-080). In advanced passages of LCO-0157, prongs were starting to extend from the organoid's body into the surrounding Matrigel. Scale bar: 100 μm . **(C):** Using a modified minimal medium, intermediate and long-term expansion of NSCLC organoids was possible. Culture day was counted from the initiation of organoid establishment (i.e., the day of surgery). Scale bar: 200 μm .

Table 2. Patient characteristics of NSCLC specimens used for primary organoid culture (n = 37).

ID	Specimen Diameter (mm)	Organoid Culture Established	Targeted Sequencing	Sex	Age	Smoking History (py)	Histology	TNM (8th Edition)	UICC Stage	Heman-giosis	Lymph-angiosis	Differen-tiation	Neoadjuvant Treatment	Surgery
LCO-63	6	Y (1)	-	f	58	35	AC	pT1b pN0 cM0	IA2	V0	L0	n/a	N	RATS lobectomy
LCO-79	15	Y (2)	wt	m	84	19	MUC	pT2b pN0 cM0	IIA	V0	L1	G3	N	RATS lobectomy
LCO-80	6	Y (3)	PIK3CA amplification	m	68	95	SCC	pT2a pN1 cM0	IIB	V1	L1	n/a	N	Open double-sleeve lobectomy
LCO-82	8	Y (4)	wt	f	82	0	AtC	pT3 pN1 pM1b	IV	V1	L1	n/a	N	RATS lobectomy
LCO-83	5	N	-	m	71	100	SCC	pT4 pN1 pM1a	IV	V0	L1	n/a	Y: Chemotherapy	VATS wedge resection (metastasis)
LCO-89	16	Y (5)	CDK4 amplification	f	69	30	AC	pT2a pN1 cM0	IIB	V1	L0	G3	N	VATS lobectomy
LCO-92	18	N	-	f	60	45	AC	pT3 pN0 cM0	IIB	V1	L0	G3	N	RATS lobectomy
LCO-97	10	Y (6)	wt	m	70	60	AC	pT1b pN0 cM0	IA2	V1	L0	G2	N	RATS lobectomy
LCO-94	4	N	-	m	62	120	AC	ypT4 ypN1 cM0	IIIA	V1	L0	n/a	Y: Radio-chemotherapy	Open lobectomy, chest wall resection
LCO-99	9	Y (7)	PIK3CA amplification	m	62	80	SCC	pT2a pN0 cM0	IB	V1	L1	G3	N	RATS lobectomy
LCO-102	4	N	-	f	75	35	AC	pT1b cN0 cM0	IA2	n/a	n/a	n/a	N	VATS wedge resection
LCO-103	8	Y (8)	-	f	77	50	AC	pT3 pN1 cM0	IIIA	V1	L1	G3	N	Open bilobectomy
LCO-106	10	Y (9)	-	m	71	50	SCC	pT1b pN0 cM0	IA2	V0	L0	G2	N	VATS lobectomy
LCO-093	12	N	-	m	73	120	SCC	pT1c pN0 cM0	IA3	V0	L0	G2	N	RATS lobectomy
LCO-110	4	N	-	m	66	30	SCC	pT2a pN1 cM0	IIA	V1	L1	G2	N	Open double-sleeve lobectomy
LCO-111	8	N	-	m	58	40	SCC	ypT3 ypN0 cM0	IIIA	V0	L1	n/a	Y: Radio-chemotherapy	Pneumonectomy
LCO-114	6	Y (10)	MET fusion	f	62	10	AC	pT3 pN0 cM0	IIB	V0	L0	G1	N	VATS lobectomy

Table 2. Cont.

ID	Specimen Diameter (mm)	Organoid Culture Established	Targeted Sequencing	Sex	Age	Smoking History (py)	Histology	TNM (8th Edition)	UICC Stage	Heman-giosis	Lymph-angiosis	Differen-tiation	Neoadjuvant Treatment	Surgery
LCO-113	15	Y (11)	-	m	71	50	SCC	pT3 pN1 cM0	IIIA	V1	L1	G3	N	VATS lobectomy
LCO-127	10	N	-	f	65	40	AC	pT4 pN0 cM0	IIIA	V1	L0	G2	N	VATS lobectomy
LCO-128	7	Y (12)	KRAS G12V mutation	m	62	40	AC	ypT4 ypN2 pM1b	IVA	n/a	n/a	n/a	Y: Chemotherapy	Open mediastinal lymphadenectomy
LCO-135	7	N	-	f	61	20	AC	pT2b pN2 cM0	IIIA	V1	L1	G2	Y: Chemotherapy	VATS lobectomy
LCO-140	6	N	-	m	71	80	PC	pT3 pN0 cM1b	IVA	V0	L0	G3	N	VATS lobectomy
LCO-141	7	N	-	f	66	40	AC	pT2a pN0 cM0	IB	V1	L0	G3	N	RATS lobectomy
LCO-145	5	N	-	f	60	40	AC	pT1c pN0 cM0	IA3	V0	L0	G2	N	RATS lobectomy
LCO-148	6	N	-	m	63	80	SCC	pT2 pN0 cM0	IB	V0	L0	G2	N	Open sleeve-lobectomy
LCO-149	5	N	-	m	62	135	SCC	pT1c pN0 cM0	IA3	V0	L0	n/a	N	Open lobectomy
LCO-153	9	N	-	f	69	0	PC	pT3 pN1 cM0	IIIA	V1	L1	G3	N	Pneumonectomy
LCO-154	8	N	-	m	74	90	SCC	pT2a pN0 cM0	IB	V1	L0	G3	N	VATS lobectomy
LCO-155	6	N	-	m	65	13	AC	pT1c pN0 cM0	IA3	V1	L0	G2	N	Pneumonectomy
LCO-157	4	Y (14)	RET imbalance	m	54	40	AtC	pT1b pN0 cM0	IA2	V0	L0	n/a	N	RATS lobectomy
LCO-158	18	N	-	f	52	30	AC	cTX pN2 cM0	IIIA	n/a	n/a	n/a	Y: Chemotherapy	Open mediastinal lymphadenectomy
LCO-166	5	Y (13)	-	m	83	1	AC	pT1c pN0 cM0	IA3	V0	L0	G2	N	RATS lobectomy
LCO-167	9	N	-	m	76	0	AC	pT1b pN2 cM0	IIIA	V0	L0	G2	N	RATS wedge resection
LCO-170	8	Y (15)	MET amplification	m	57	40	AC	pT1b pN1 cM0	IIB	V1	L1	G2	N	VATS lobectomy
LCO-275	9	Y (16)	wt	f	77	50	SCC	pT2b pN0 cM0	IIA	V1	L0	G2	N	VATS lobectomy
LCO-279	6	Y (17)	EGFR Ex20Ins	f	56	15	AC	pT2a pN0 cM0	IB	V0	L0	G2	N	VATS lobectomy
LCO-283	18	Y (18)	KRAS G12C mutation	f	55	25	AC	pT4 pN1 cM0	IIIB	V1	L0	G3	Y: Chemotherapy	Open lobectomy

AC: adenocarcinoma, amp: amplification, AtC: atypical carcinoid, LAD: lymphadenectomy, MUC: mucoepidermoid carcinoma, mut: mutation, PC: pleomorphic carcinoma, RATS: robotic-assisted thoracoscopic surgery, SCC: squamous cell carcinoma, VATS: video-assisted thoracoscopic surgery.

3.2. Histological and Immunohistochemical Characterization of NSCLC Organoids

Organoids derived from SCC showed polygonal cells, nuclear pleomorphism, hyperchromasia, and brightly eosinophilic cytoplasm suggesting intracellular keratinization. Upon IHC, cells were TTF-1-negative, p40-positive and panCK-positive (Figure 3A). Organoids derived from AC displayed abundant cytoplasm with mucin. Expression of TTF-1 was often less dominant than in the primary tumor. p40 IHC remained negative, and panCK expression was retained. Among AC organoids, the formation of cystic spheres was more commonly encountered when compared to SCC organoids (Figure 3B). Organoids established from a case of mucoepidermoid carcinoma reflected the characteristic mixed histology of the parental tissue with both p40-positive and -negative tumor cells (Figure 3C). Organoids derived from carcinoid tumor tissue showed morphological features of the parental pulmonary carcinoid tumor including granular chromatin and growth in confluent tumor cell nests (Figure 3D). IHC revealed a strong positivity for TTF-1 and synaptophysin and no expression of p40 in both parental tissue and organoids. While the Ki-67 proliferation index was low (1.5%) in the primary tumor of the specimen depicted in Figure 3D (LCO-157), the derived organoids displayed a substantially increased index of 70%, suggesting a selection of a subunit of rapidly growing neuroendocrine cells. IHC furthermore confirmed the maintenance of intratumoral heterogeneity among the established organoids; partial and heterogeneous p40 expression and a heterogeneous expression of CD44 demonstrated variability in the differentiation, stemness, and proliferative capacity of lung cancer cells within the organoid (Figure 4).

3.3. Genetic Characterization by NGS

For genetic characterization of established organoids, NGS was first performed on parental tumor tissue to determine whether traceable aberrations were present. Overall, 13 out of 18 established organoids offered sufficient organoid tissue to perform NGS. Targeted sequencing revealed traceable genetic aberrations in nine parental tumors, whereas four parental tumors showed a wild-type status (Table 2). The parental tumor's oncogenic driver mutation was maintained in three out of nine organoid cultures and included a KRAS p.Gly12Val mutation in a stage IV AC, a KRAS p.Gly12Cys mutation in a stage IIIB AC, and an RET-fusion in a stage IA2 typical carcinoid (Figure 5). In the other six organoids, the parental tumor's genetic alteration was lost, and copy number variations (CNVs) were not retained in our cohort.

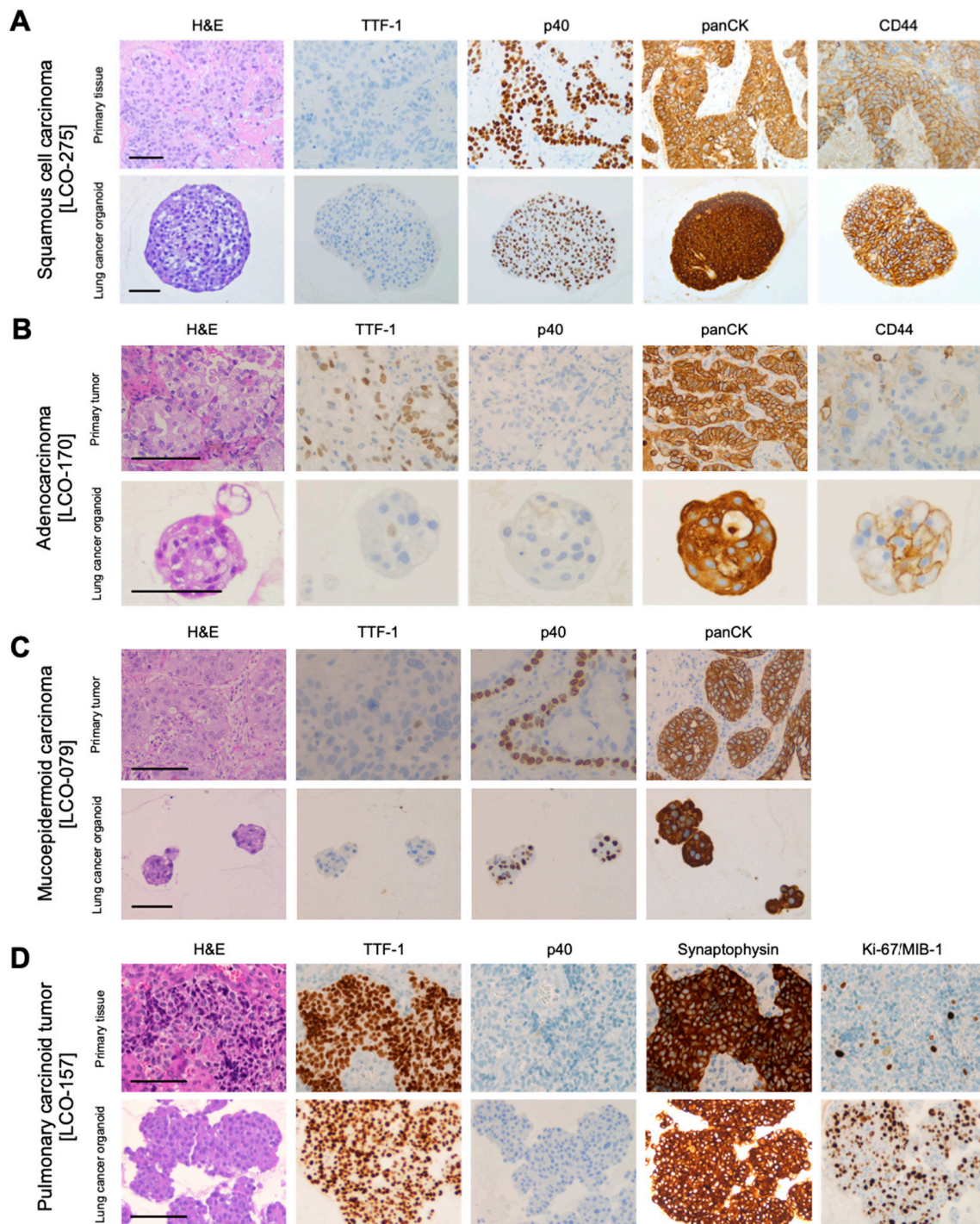


Figure 3. Morphological and immunohistochemical characteristics of primary NSCLC organoids and their respective parental tissue. (A): Lung squamous cell carcinoma with intracellular keratinization, intercellular bridges and strong expression of p40 and CD44. (B): Lung adenocarcinoma with intracellular mucin and an increased expression of CD44 in the organoid. (C): TTF-1-negative mucoepidermoid carcinoma organoids with characteristic mixed histology, including p40-positive and p40-negative cells. (D): Typical carcinoid tumor with growth in tumor cell nests and strong positivity for TTF-1 and synaptophysin. The Ki-67 proliferation index was notably increased from 1.5% in the parental tissue to 70% in the derived organoid. Scale bar: 100 μ m.

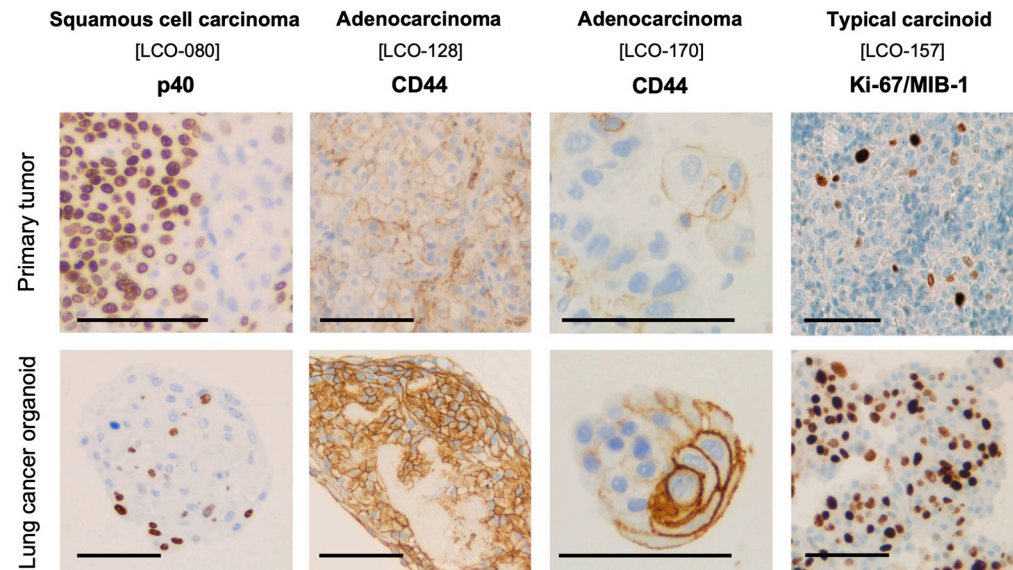


Figure 4. NSCLC organoids derived from squamous cell carcinoma LCO-080 maintain the parental tumor's heterogeneous expression of p40. Organoids derived from adenocarcinomas LCO-128 and LCO-170 show an increased but heterogeneous expression of CD44 when compared to the primary tumor. Ki-67 is upregulated, but heterogeneously expressed in organoids derived from the typical carcinoid LCO-157. Scale bar: 100 μ m.

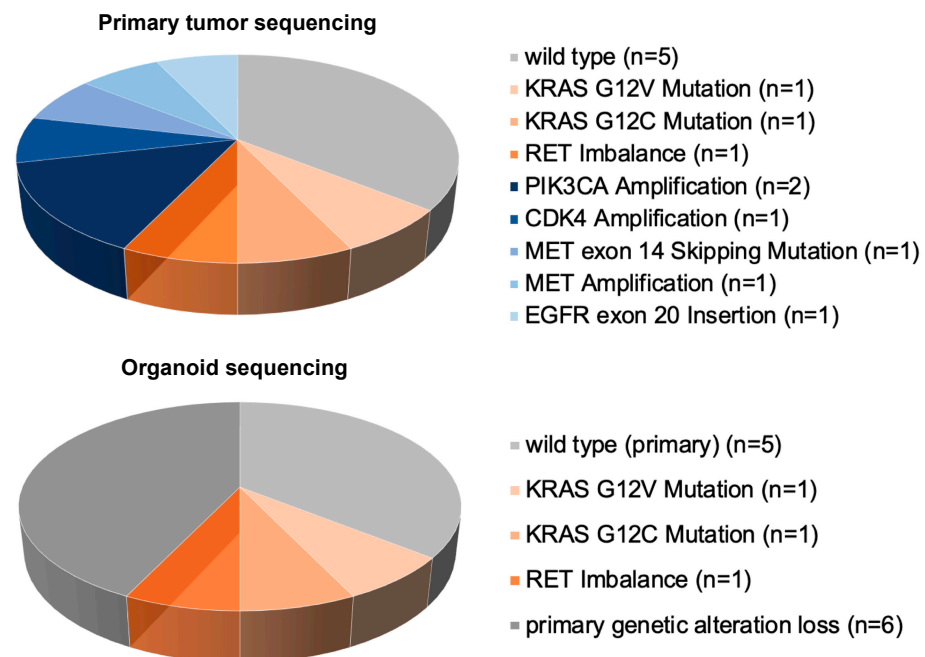


Figure 5. Targeted sequencing of the primary tumor (**top**) and the organoids (**bottom**). Genetic aberrations were detected in nine primary tumors. In one-third of the established organoids, the primary tumor's oncogenic driver was preserved, including a KRAS G12V mutation, a KRAS G12C mutation, and an RET imbalance.

4. Discussion

For a personalized approach to cancer treatment, patient-derived in vitro models are required. Such models should faithfully represent the morphological and genetic characteristics as well as the heterogeneity of the parental tumors. Newly developed three-dimensional organoid cultures are the up-and-coming platforms for disease modeling.

Primary organoid models with the ability to self-organize and to maintain the parental tumor's complex composition allow us to mimic the pathophysiology of cancer more closely than conventional two-dimensional cell lines, since the long-term manipulation of immortalized cell lines alters phenotype, diversity, and function of cells [7]. The growing clinical potential of three-dimensional primary cancer cultures as patient avatars for disease-specific drug screening has recently been shown in high-throughput screening studies on colon cancer and melanoma [15,16].

Using a modified minimal medium formulation and a commercially available extracellular matrix, we successfully established and validated primary NSCLC organoids from four different histological subtypes including all four UICC-stages. In order to avoid a selection for TP53-mutated organoids by using a Nutlin-3a-based medium, we used a minimal medium formulation that lacks essential growth factors for normal airway epithelium culture. Following a learning curve, intermediate-term expansion was achieved with organoids surviving up to 10 passages and 2–3 months in culture. The characteristic morphological and immunohistochemical features of the parental tumor were maintained in the organoids, and spatial self-organization was evident. In addition, oncogenic drivers such as KRAS mutations and an RET imbalance were maintained in selected organoids.

Our culture protocol allows for the fast and cost-efficient formation of primary NSCLC organoids. Among the 18 organoids established in this study, a higher establishment rate was seen in AC organoids (50.0%) when compared to SCC organoids (41.6%), although this was based on small sample sizes. Apart from histotype, no correlation between a successful culture and the clinical parameters of cancer aggressiveness, such as TNM staging or tumor grading score, was apparent. However, the tumor quality appeared to be essential for successful organoid growth. After neoadjuvant treatment, tumor specimens supposedly lacked enough viable cells to drive organoid growth. In contrast, specimens from patients who had not undergone previous treatment often showed good organoid-forming potential despite a limited amount of tissue. In our study, we aimed to include and culture all NSCLC specimens irrespective of previous treatments to gain an overview of the “real-life” success rate which is to be expected in a clinical setting. Our establishment rate of 48.6% matches previously reported results by Herreros-Pomares et al. [17] but does not equal the high success rates of 70% and 88% reported by Kim et al. and Shi et al. [9,13]. However, genetic characterization by NGS revealed that oncogenic drivers of the parental tumor are only preserved in one third of all organoids, suggesting that a selective outgrowth of tumor subclones or a rapid tumor evolution is common. Comparable to our findings, the studies conducted by Dijkstra et al. and Sachs et al. also reported low establishment rates of genetically validated organoids with 12% and 28%, respectively [8,10]. To identify where the divergence occurs and whether subclonal mutations are as well preserved, further studies including whole-genome sequencing of organoids are required [18]. This will additionally allow us to validate the cases with alterations that were not part of the targeted NGS panel used in our cohort. The loss of certain mutations among our cohort of organoids (e.g., MET exon 14 skipping mutation and EGFR exon 20 insertion) further raises the question as to whether these alterations were indeed the driving forces of cancer growth.

With the growing application of targeted treatments in locally advanced or metastatic NSCLC, the preservation of the oncogenic drivers in primary organoids is essential. Our findings also demonstrate that histomorphological and immunohistochemical validation alone are not sufficient for a faithful validation of primary NSCLC organoids. Genetic validation by NGS or CNV analysis should therefore always be performed before organoids are used for clinical purposes. With current establishment rates, patient-derived NSCLC organoids are not yet ready for widespread clinical application in precision medicine, and efforts should thus be made to increase the establishment rate of genetically validated organoids. In the light of the broad genetic heterogeneity of NSCLC, a personalized mutation-directed approach to organoid culture may be a promising strategy to enhance organoid establishment. Considering the limited growth in specimens from pre-treated

patients, we recommend that future co-clinical trials focus on treatment-naïve patients in order to enhance organoid establishment.

The development of dynamic changes and selection of certain subpopulations have been previously reported in organoids from various types of cancer after serial passaging [7] and also occurred in the NSCLC organoids established in this study. This included the selection of fast-proliferating neuroendocrine cells derived from a typical carcinoid, resulting in a substantially increased Ki-67/MIB-1 proliferation index of 70%, or the selection of AC cells expressing CD44 as a marker of cancer stemness [19]. Similarly, Herreros-Pomares and colleagues have also reported an increased expression of stem cell-associated genes, including CD44, in tumorspheres from primary lung AC samples [17]. Due to this known gain in clonality after serial passaging, drug screenings and other clinical applications should be performed on early-passage organoids, since they resemble the parental tumor most closely [7].

This study is subject to limitations that need to be considered. First, it must be highlighted that despite histomorphological, immunohistochemical and genetic validation, organoids remain a reductionist model [18]. While the complex tumor microenvironment is known to contribute to tumorigenesis and treatment response, it remains to be investigated whether isolated NSCLC organoid models can nevertheless recapitulate clinical treatment scenarios. Second, the number of organoids established does not allow for a statistical correlation of clinical outcomes and parameters of cancer aggressiveness with culture success or characteristics of organoid growth. Further studies are required to assess the predictive value of parameters of organoid growth. Second, the established organoids are only able to mimic their originating specimen. A faithful representation of the entire intratumoral heterogeneity therefore also requires a representative specimen, ideally by multiple biopsies from different tumor regions. In our study, we aimed to overcome this issue by cutting the received specimen into a homogeneous mass and thereby creating an even distribution of these diverse characteristics.

Despite these limitations, the results obtained in this study are in line with previous studies into NSCLC organoids [8–11,13], confirming the general feasibility of establishing representative organoids of different NSCLC subtypes, including a histological and genetic characterization.

5. Conclusions

In summary, our study demonstrates that patient-derived NSCLC organoids can be established from fresh cancer tissue specimens and can maintain the central morphological, immunohistochemical, and genetic characteristics of their parental tumor. As parental oncogenic drivers were only preserved in one-third of the established organoids, genetic validation should always be performed before organoids are used for clinical purposes. Furthermore, the early selection of proliferative or pluripotent cancer cells under culture conditions highlights the value of early organoids for drug screening, as they resemble the primary tumor's characteristics most closely. We expect that primary NSCLC organoids will find broad applications in translational and co-clinical projects aiming to identify novel cancer treatment candidates.

Supplementary Materials: The following supporting information can be downloaded at: <https://www.mdpi.com/article/10.3390/organoids3040017/s1>, Table S1: Characteristics of successful and failed organoid establishment.

Author Contributions: Conceptualization: R.S.W., M.B.K. and I.O.; Methodology: all authors; Software: R.S.W.; Validation: R.S.W., M.B.K. and I.O.; Formal analysis: R.S.W., M.B.K. and M.R.; Investigation: R.S.W., J.-H.J. and M.B.K.; Resources: M.B.K. and I.O.; Data curation: R.S.W. and M.B.K.; Writing—original draft: R.S.W.; Writing—review and editing: R.S.W., J.-H.J., M.B.K., M.R. and I.O.; Visualization: R.S.W.; Supervision: M.B.K. and I.O.; Project administration: R.S.W., J.-H.J. and M.B.K.; Funding acquisition: R.S.W., J.-H.J., M.B.K. and I.O. All authors have read and agreed to the published version of the manuscript.

Funding: This study was funded by the Iten-Kohaut Foundation, the Kurt und Senta Herrmann Foundation, and the Stiftung für angewandte Krebsforschung (SAKF) Zurich (SAKF F-86901-70-01).

Institutional Review Board Statement: This study was conducted in accordance with the Declaration of Helsinki and approved by the Cantonal Ethics Committee of Zurich (BASEC-reference number: 2019-01313, approved 4 September 2019).

Informed Consent Statement: Informed consent was obtained from all subjects involved in the study.

Data Availability Statement: The data underlying this article will be shared on reasonable request to the corresponding author.

Acknowledgments: We acknowledge the Iten-Kohaut Foundation, the Kurt und Senta Herrmann Foundation, and the Stiftung für angewandte Krebsforschung (SAKF) Zurich for funding support, without which this study would not have been possible. We would also like to thank Susanne Dettwiler for coordination and help with the timely transfer of NSCLC tissue to the laboratory.

Conflicts of Interest: Jae-Hwi Jang, Markus Rechsteiner and Michaela B. Kirschner have no conflicts of interest. Raphael S. Werner has no real conflicts of interest. The following could be perceived as such: BMS (Advisory Board) and MSD (Advisory Board). Isabelle Opitz has no real conflicts of interest. The following could be perceived as such: Roche (Institutional Grant and Speakers Fee), Roche Genentech (Steering Committee), AstraZeneca (Advisory Board and Speakers Fee), MSD (Advisory Board), BMS (Advisory Board), Medtronic (Institutional Grant and Advisory Board), and Intuitive (Proctorship).

Abbreviations

AC	Adenocarcinoma
bFGF	Basic fibroblast growth factor
CNV	Copy number variation
DPBS	Dulbecco's phosphate-buffered saline
EGFR	Epidermal growth factor receptor
hEGF	Human epidermal growth factor
H&E	Hematoxylin and eosin
IHC	Immunohistochemistry
KRAS	Kirsten rat sarcoma virus
NGS	Next-generation sequencing
NSCLC	Non-small cell lung cancer
panCK	Pan-cytokeratin
PDX	Patient-derived xenograft
SCC	Squamous cell carcinoma
TTF-1	Thyroid transcription factor-1
UICC	Union for International Cancer Control

References

1. Wild, C.; Weiderpass, E.; Steward, B. *World Cancer Report: Cancer Research for Cancer Prevention*; International Agency for Research on Cancer: Lyon, France, 2020.
2. Jamal-Hanjani, M.; Wilson, G.A.; McGranahan, N.; Birkbak, N.J.; Watkins, T.B.; Veeriah, S.; Swanton, C. Tracking the Evolution of Non-Small-Cell Lung Cancer. *N. Engl. J. Med.* **2017**, *376*, 2109–2121. [[CrossRef](#)] [[PubMed](#)]
3. Gazdar, A.F.; Girard, L.; Lockwood, W.W.; Lam, W.L.; Minna, J.D. Lung cancer cell lines as tools for biomedical discovery and research. *J. Natl. Cancer Inst.* **2010**, *102*, 1310–1321. [[CrossRef](#)] [[PubMed](#)]
4. Zheng, S.; El-Naggar, A.K.; Kim, E.S.; Kurie, J.M.; Lozano, G. A genetic mouse model for metastatic lung cancer with gender differences in survival. *Oncogene* **2007**, *26*, 6896–6904. [[CrossRef](#)] [[PubMed](#)]
5. Wang, D.; Pham, N.A.; Tong, J.; Sakashita, S.; Allo, G.; Kim, L.; Tsao, M.S. Molecular heterogeneity of non-small cell lung carcinoma patient-derived xenografts closely reflect their primary tumors. *Int. J. Cancer* **2017**, *140*, 662–673. [[CrossRef](#)] [[PubMed](#)]
6. Gillet, J.P.; Varma, S.; Gottesman, M.M. The clinical relevance of cancer cell lines. *J. Natl. Cancer Inst.* **2013**, *105*, 452–458. [[CrossRef](#)] [[PubMed](#)]
7. Lo, Y.-H.; Karlsson, K.; Kuo, C.J. Applications of organoids for cancer biology and precision medicine. *Nat. Cancer* **2020**, *1*, 761–773. [[CrossRef](#)] [[PubMed](#)]

8. Sachs, N.; Papaspyropoulos, A.; Zomer-van Ommen, D.D.; Heo, I.; Böttinger, L.; Klay, D.; Clevers, H. Long-term expanding human airway organoids for disease modeling. *EMBO J.* **2019**, *38*, e100300. [[CrossRef](#)] [[PubMed](#)]
9. Kim, M.; Mun, H.; Sung, C.O.; Cho, E.J.; Jeon, H.J.; Chun, S.M.; Jung, D.J.; Shin, T.H.; Jeong, G.S.; Kim, D.K.; et al. Patient-derived lung cancer organoids as in vitro cancer models for therapeutic screening. *Nat. Commun.* **2019**, *10*, 3991. [[CrossRef](#)] [[PubMed](#)]
10. Dijkstra, K.K.; Monkhorst, K.; Schipper, L.J.; Hartemink, K.J.; Smit, E.F.; Kaing, S.; de Groot, R.; Wolkers, M.C.; Clevers, H.; Cuppen, E.; et al. Challenges in Establishing Pure Lung Cancer Organoids Limit Their Utility for Personalized Medicine. *Cell Rep.* **2020**, *31*, 107588. [[CrossRef](#)] [[PubMed](#)]
11. Li, Z.; Qian, Y.; Li, W.; Liu, L.; Yu, L.; Liu, X.; Wu, G.; Wang, Y.; Luo, W.; Fang, F.; et al. Human Lung Adenocarcinoma-Derived Organoid Models for Drug Screening. *iScience* **2020**, *23*, 101411. [[CrossRef](#)] [[PubMed](#)]
12. Werner, R.S.; Kirschner, M.B.; Opitz, I. Primary Lung Cancer Organoids for Personalized Medicine—Are They Ready for Clinical Use? *Cancers* **2021**, *13*, 4832. [[CrossRef](#)] [[PubMed](#)]
13. Shi, R.; Radulovich, N.; Ng, C.; Liu, N.; Notsuda, H.; Cabanero, M.; Martins-Filho, S.N.; Raghavan, V.; Li, Q.; Mer, A.S.; et al. Organoid Cultures as Preclinical Models of Non-Small Cell Lung Cancer. *Clin. Cancer Res.* **2020**, *26*, 1162–1174. [[CrossRef](#)] [[PubMed](#)]
14. Yatabe, Y.; Dacic, S.; Borczuk, A.C.; Warth, A.; Russell, P.A.; Lantuejoul, S.; Beasley, M.B.; Thunnissen, E.; Pelosi, G.; Rekhtman, N.; et al. Best Practices Recommendations for Diagnostic Immunohistochemistry in Lung Cancer. *J. Thorac. Oncol.* **2019**, *14*, 377–407. [[CrossRef](#)] [[PubMed](#)]
15. Boehnke, K.; Iversen, P.W.; Schumacher, D.; Lallena, M.J.; Haro, R.; Amat, J.; Haybaeck, J.; Liebs, S.; Lange, M.; Schäfer, R.; et al. Assay Establishment and Validation of a High-Throughput Screening Platform for Three-Dimensional Patient-Derived Colon Cancer Organoid Cultures. *J. Biomol. Screen.* **2016**, *21*, 931–941. [[CrossRef](#)] [[PubMed](#)]
16. Rebecca, V.W.; Somasundaram, R.; Herlyn, M. Pre-clinical modeling of cutaneous melanoma. *Nat. Commun.* **2020**, *11*, 2858. [[CrossRef](#)] [[PubMed](#)]
17. Herreros-Pomares, A.; de-Maya-Girones, J.D.; Calabuig-Fariñas, S.; Lucas, R.; Martínez, A.; Pardo-Sánchez, J.M.; Camps, C. Lung tumorspheres reveal cancer stem cell-like properties and a score with prognostic impact in resected non-small-cell lung cancer. *Cell Death Dis.* **2019**, *10*, 660. [[CrossRef](#)] [[PubMed](#)]
18. Hughes, T.; Dijkstra, K.K.; Rawlins, E.L.; Hynds, R.E. Open questions in human lung organoid research. *Front. Pharmacol.* **2022**, *13*, 1083017. [[CrossRef](#)] [[PubMed](#)]
19. Wang, L.; Zuo, X.; Xie, K.; Wei, D. The Role of CD44 and Cancer Stem Cells. *Methods Mol. Biol.* **2018**, *1692*, 31–42. [[CrossRef](#)] [[PubMed](#)]

Disclaimer/Publisher’s Note: The statements, opinions and data contained in all publications are solely those of the individual author(s) and contributor(s) and not of MDPI and/or the editor(s). MDPI and/or the editor(s) disclaim responsibility for any injury to people or property resulting from any ideas, methods, instructions or products referred to in the content.